Pion mass dependence of the nucleon form factors of the energy-momentum tensor in the chiral quark-soliton model

K. Goeke,[1] J. Grabis,[1] J. Ossmann,[1] P. Schweitzer,[1] A. Silva,[2,3] and D. Urbano[2,3]
[1]*Institut für Theoretische Physik II, Ruhr-Universität Bochum, D-44780 Bochum, Germany*
[2]*Centro de Física Computacional (CFC), Departamento de Física, Universidade de Coimbra, P-3004-516 Coimbra, Portugal*
[3]*Faculdade de Engenharia da Universidade do Porto, P-4200-465 Porto, Portugal*
(Received 1 March 2007; published 23 May 2007)

The nucleon form factors of the energy-momentum tensor are studied in the large-N_c limit in the framework of the chiral quark-soliton model for model parameters that simulate physical situations in which pions are heavy. This allows for a direct comparison to lattice quantum chromodynamics results.

DOI: 10.1103/PhysRevC.75.055207 PACS number(s): 13.60.Hb, 12.39.Fe, 12.38.Gc

I. INTRODUCTION

The nucleon energy-momentum tensor (EMT) form factors [1] contain valuable information on the nucleon structure. They carry information on, e.g., how the quark and gluon degrees of freedom share the total momentum, angular momentum of the nucleon [2], or on the distribution of strong forces inside the nucleon [3]. The first is known from deeply inelastic lepton nucleon scattering experiments. The latter two can be deduced from generalized parton distribution functions (GPDs) [4–7] accessible in hard exclusive reactions [8–16]; see Refs. [17–23] for reviews.

Nucleon EMT form factors were studied in lattice quantum chromodynamics (QCD) calculations [24–28]. In principle, lattice QCD provides a rigorous and model-independent approach to compute the nucleon EMT form factors. In practice, however, present-day technics and computing power allow to simulate on lattices "worlds" with pions of typically $m_\pi \gtrsim 400\,\mathrm{MeV}$. The situation is expected to improve in the future, see Ref. [29] for status reports on selected topics.

For the time being, however, it is necessary to use chiral extrapolation to relate lattice results to the real-world situation. Chiral perturbation theory (χPT) provides a model-independent tool for that, and the chiral behavior of the nucleon EMT form factors was studied in Refs. [30–32]. Experience with chiral extrapolations of other nucleon properties indicates that χPT is applicable up to the lowest presently available lattice values of m_π [33–35], although the issue is not yet settled [36].

In this situation it is worth looking at what one can learn about the chiral behavior of nucleon properties from other effective approaches, e.g., the "finite range regulator" (FRR) approach. There chiral loops are regulated by suitably chosen vertex form factors to phenomenologically simulate the effects of the pion cloud that has a finite range due to $m_\pi \neq 0$ [37,38]. However, model calculations [39–41] are equally of interest in this context.

A phenomenologically successful and theoretically consistent model for the description of nucleon properties *at the physical point* and *in the chiral limit*, is the chiral quark soliton model (CQSM) [42,43]. This model describes the nucleon as a soliton of a static background pion field in the limit of a large number of colours, N_c, and hence provides a particular realization of the general large-N_c picture of the nucleon [44]. The CQSM describes numerous nucleonic properties without adjustable parameters—including among others form factors [45–48], usual parton distribution functions [49–53] and GPDs [54–59]—within an accuracy of (10–30)% as far as those quantities are known.

That it is possible to extend the CQSM to the description of the nucleon at *large pion masses* was shown in Ref. [41], where the model was demonstrated to provide a good description of lattice data on the m_π dependence of the nucleon mass M_N up to $m_\pi \lesssim 1.5\,\mathrm{GeV}$. An important prerequisite for that is that the CQSM formally contains the correct heavy quark limit result for the nucleon mass M_N [41].

In this work we present a study of the m_π dependence of the nucleon EMT form factors in the CQSM up to pion masses as large as 1 GeV. The present study extends the study of Ref. [60], where the nucleon EMT form factors were studied at the physical point and in the chiral limit, and its purpose is threefold.

First, we provide an important supplement for the study in Ref. [41]. There soliton solutions were obtained numerically for model parameters corresponding to pion masses in the range $0 \leqslant m_\pi \leqslant 1.5\,\mathrm{GeV}$. Here we provide a cross-check demonstrating that the numerical solutions found in Ref. [41] correspond, in fact, to stable solitons.

Second, with the results obtained for large m_π we are in the position to confront the model predictions for the nucleon EMT form factors directly to lattice QCD results [24–28]. In view of the early stage of art of the experimental situation of hard exclusive reactions, such a comparison provides the only presently available test for our results.

Third, though the model—as discussed in detail in Ref. [41]—cannot be used as a quantitative guideline for the chiral extrapolation, our study still allows us to gain several interesting qualitative insights with this respect.

It should be mentioned that the general chiral structure of the EMT was studied in chiral perturbation theory and/or chiral models in Refs. [61–63], and aspects of pion EMT form factors in lattice QCD were discussed in Refs. [64,65].

The article is organized as follows. In Sec. II we introduce the nucleon EMT form factors and discuss their properties. In Sec. III we briefly review how the nucleon EMT form factors are described in the CQSM. In Secs. IV and V we describe

respectively the model results for the densities associated with the form factors and the form factors themselves. In Sec. VI we compare the model results with lattice QCD data, and in Sec. VII we discuss which qualitative observations from our study could be of interest in the context of the chiral extrapolation of lattice data. Section VIII contains the conclusions. A remark on different notations for the EMT form factors is posed in Appendix.

II. FORM FACTORS OF THE ENERGY-MOMENTUM TENSOR

The nucleon matrix element of the symmetric EMT of QCD is characterized by three scalar form factors [1]. The quark and gluon parts, $\hat{T}^{Q}_{\mu\nu}$ and $\hat{T}^{G}_{\mu\nu}$, of the EMT are separately gauge invariant and can be parametrized as, see Refs. [2,3] and cf. Appendix for an alternative notation,

$$\begin{aligned}\langle p'|\hat{T}^{Q,G}_{\mu\nu}(0)|p\rangle &= \bar{u}(p')\left[M_2^{Q,G}(t)\,\frac{P_\mu P_\nu}{M_N} + J^{Q,G}(t)\frac{i(P_\mu\sigma_{\nu\rho}+P_\nu\sigma_{\mu\rho})\Delta^\rho}{2M_N}\right.\\ &\left. + d_1^{Q,G}(t)\frac{\Delta_\mu\Delta_\nu - g_{\mu\nu}\Delta^2}{5M_N} \pm \bar{c}(t)g_{\mu\nu}\right]u(p). \qquad (1)\end{aligned}$$

Here the nucleon states and spinors are normalized by $\langle p'|p\rangle = 2p^0(2\pi)^3\delta^{(3)}(\mathbf{p}'-\mathbf{p})$ and $\bar{u}(p)u(p) = 2M_N$, and spin indices are suppressed for brevity. The kinematical variables are defined as $P = (p+p')/2$, $\Delta = (p'-p)$, $t = \Delta^2$. The form factor $\bar{c}(t)$ accounts for nonconservation of the separate quark and gluon parts of the EMT, and enters the quark and gluon parts with opposite signs such that the total (quark+gluon) EMT is conserved.

The nucleon form factors of the EMT are related to the second Mellin moments of the unpolarized GPDs $H^f(x,\xi,t)$ and $E^f(x,\xi,t)$ as (we use the notation of Ref. [19])

$$\begin{aligned}\int_{-1}^{1} dx\, x \sum_f H^f(x,\xi,t) &= M_2^Q(t) + \frac{4}{5}d_1^Q(t)\xi^2,\\ \int_{-1}^{1} dx\, x \sum_f (H^f + E^f)(x,\xi,t) &= 2J^Q(t). \qquad (2)\end{aligned}$$

where ξ denotes the so-called skewedness parameter [2]. The sum rules in Eqs. (2) are special cases of the so-called polynomiality property of GPDs [17]. The second sum rule in (2) provides the possibility to access $J^Q(0)$, i.e., the total (spin+orbital angular momentum) contribution of quarks to the nucleon spin, through the extraction of GPDs from hard exclusive processes and extrapolation to the unphysical point $t = 0$. The sensitivity of different observables to the total quark angular momenta was investigated in model studies [19,66]. For gluons there are analog definitions and expressions. Suffice to remark that the full GPDs contain far more information [23].

The form factors of the EMT in Eq. (1) can be interpreted [3] in analogy to the electromagnetic form factors [67] in the Breit frame characterized by $\Delta^0 = 0$. In this frame one can define the static energy-momentum tensor for quarks

$$T^Q_{\mu\nu}(\mathbf{r},\mathbf{s}) = \frac{1}{2E}\int \frac{d^3\mathbf{\Delta}}{(2\pi)^3}\,\exp(i\,\mathbf{\Delta r})\langle p', S'|\hat{T}^Q_{\mu\nu}(0)|p, S\rangle, \qquad (3)$$

and analogously for gluons. The initial and final polarization vectors of the nucleon S and S' are defined such that in the respective rest-frame they are equal to $(0,\mathbf{s})$ with the unit vector $\mathbf{s}$ denoting the quantization axis for the spin.

The components of $T^Q_{0k}(\mathbf{r},\mathbf{s})$ and $\varepsilon^{ijk}r_j T^Q_{0k}(\mathbf{r},\mathbf{s})$ correspond, respectively, to the distribution of quark momentum and quark angular momentum inside the nucleon. The components of $(T^Q_{ik} - \frac{1}{3}\delta_{ik}T^Q_{ll})(\mathbf{r},\mathbf{s})$ characterize the spatial distribution of "shear forces" experienced by quarks inside the nucleon. The respective form factors are related to $T^Q_{\mu\nu}(\mathbf{r},\mathbf{s})$ by

$$\begin{aligned}J^Q(t) + \frac{2t}{3}J^{Q\prime}(t) &= \int d^3\mathbf{r} e^{-i\mathbf{r\Delta}}\,\varepsilon^{ijk}\,s_i\,r_j\,T^Q_{0k}(\mathbf{r},\mathbf{s}), \qquad (4)\\ d_1^Q(t) + \frac{4t}{3}d_1^{Q\prime}(t) + \frac{4t^2}{15}d_1^{Q\prime\prime}(t) &= -\frac{M_N}{2}\int d^3\mathbf{r}\, e^{-i\mathbf{r\Delta}}T^Q_{ij}(\mathbf{r})\left(r^i r^j - \frac{\mathbf{r}^2}{3}\delta^{ij}\right), \qquad (5)\\ M_2(t) - \frac{t}{4M_N^2}\left(M_2(t) - 2J(t) + \frac{4}{5}d_1(t)\right) &= \frac{1}{M_N}\int d^3\mathbf{r} e^{-i\mathbf{r\Delta}}T_{00}(\mathbf{r},\mathbf{s}), \qquad (6)\end{aligned}$$

where the prime denotes derivative with respect to the Mandelstam variable t. Note that for a spin-1/2 particle only the $T^{0\mu}$ components are sensitive to the polarization vector. Note also that Eq. (6) holds for the sum $T_{00} \equiv T^Q_{00} + T^G_{00}$ with $M_2(t) \equiv M_2^Q(t) + M_2^G(t)$ and $J(t)$ and $d_1(t)$ defined analogously, but not for the separate quark and gluon contributions—since otherwise the form factor $\bar{c}(t)$ would not cancel out.

The form factor $M_2(t)$ at $t = 0$ is connected to the fractions of the nucleon momentum carried, respectively, by quarks and gluons. More precisely

$$\begin{aligned}M_2^Q(0) &= \int_0^1 dx \sum_q x\left(f_1^q + f_1^{\bar{q}}\right)(x),\\ M_2^G(0) &= \int_0^1 dx\, x f_1^g(x), \qquad (7)\end{aligned}$$

where $f_1^a(x) = H^a(x,0,0)$ are the unpolarized parton distributions accessible in inclusive deeply inelastic scattering.

The form factors $M_2^{Q,G}(t)$, $J^{Q,G}(t)$, and $d_1^{Q,G}(t)$ are renormalization scale dependent (the indication of the renormalization scale μ is suppressed for brevity). Their quark+gluon sums, however, are scale-independent form factors, which at

$t = 0$ satisfy the constraints,

$$M_2(0) = \frac{1}{M_N}\int \mathrm{d}^3\mathbf{r}\; T_{00}(\mathbf{r},\mathbf{s}) = 1,$$
$$J(0) = \int \mathrm{d}^3\mathbf{r}\; \varepsilon^{ijk}\, s_i\, r_j\, T_{0k}(\mathbf{r},\mathbf{s}) = \frac{1}{2}, \qquad (8)$$
$$d_1(0) = -\frac{M_N}{2}\int \mathrm{d}^3\mathbf{r}\; T_{ij}(\mathbf{r})\left(r^i r^j - \frac{\mathbf{r}^2}{3}\,\delta^{ij}\right) \equiv d_1,$$

which mean that in the rest frame the total energy of the nucleon is equal to its mass and that its spin is 1/2. The value of d_1 is not known a priori and must be determined experimentally. However, being a conserved quantity it is to be considered on the same footing as other basic nucleon properties like mass, anomalous magnetic moment, etc. Remarkably, d_1 determines the behavior of the D term [68] (and thus the unpolarized GPDs) in the asymptotic limit of renormalization scale $\mu \to \infty$ [19].

The form factor $d_1(t)$ is connected to the distribution of pressure and shear forces experienced by the partons in the nucleon [3], which becomes apparent by recalling that $T_{ij}(\mathbf{r})$ is the static stress tensor that (for spin 0 and 1/2 particles) can be decomposed as

$$T_{ij}(\mathbf{r}) = s(r)\left(\frac{r_i r_j}{r^2} - \frac{1}{3}\,\delta_{ij}\right) + p(r)\,\delta_{ij}. \qquad (9)$$

Hereby $p(r)$ describes the radial distribution of the "pressure" inside the hadron, whereas $s(r)$ is related to the distribution of the "shear forces" [3]. Both are related due to the conservation of the EMT by the differential equation

$$\frac{2}{3}\,\frac{\partial s(r)}{\partial r} + \frac{2s(r)}{r} + \frac{\partial p(r)}{\partial r} = 0. \qquad (10)$$

Another important consequence of the conservation of the EMT is the so-called stability condition

$$\int_0^\infty \mathrm{d}r\; r^2 p(r) = 0. \qquad (11)$$

Let us review briefly what is known about d_1—which in terms of the pressure or shear forces is given by

$$d_1 = -\frac{1}{3}\,M_N\int \mathrm{d}^3\mathbf{r}\; r^2 s(r) = \frac{5}{4}\,M_N\int \mathrm{d}^3\mathbf{r}\; r^2 p(r). \qquad (12)$$

For the pion it can be calculated exactly using soft pion theorems with the result $\frac{4}{5}d_{1,\pi}^Q = -M_{2,\pi}^Q$ [68], see also Ref. [69]. Also for the nucleon $d_1^Q < 0$ was found in calculations in CQSM [54,60,70]. For the nucleon the large-N_c limit predicts the flavour-dependence $|d_1^u + d_1^d| \gg |d_1^u - d_1^d|$ [19]. Lattice calculations [24–28] confirm this flavour dependence and yield a negative d_1^Q, see Sec. VI. In a simple "liquid drop" model d_1 can be related to the surface tension of the "liquid" and comes out negative [3]. Such a model is in particular applicable to nuclei and predictions from this picture [3] were confirmed in calculations assuming realistic nuclear models [71]. Noteworthy, data from HERMES [12,16] favour a negative d_1^Q though this observation depends to some extent on the model for the small-x behavior of GPDs [20]. In Ref. [60] it was conjectured on the basis of plausible physical arguments that the negative sign of d_1 is dictated by stability criteria. This conclusion, however, remains to be proven for the general case.

III. NUCLEON EMT FORM FACTORS IN THE CQSM

The effective theory underlying the CQSM was derived from the instanton model of the QCD vacuum [72–74], which assumes that the basic properties of the QCD vacuum are dominated by a strongly interacting but dilute instanton medium; see the reviews [75]. In this medium light quarks acquire a dynamical ("constituent") quark mass due to interactions with instantons. At low momenta below a scale set by $\rho_{\mathrm{av}}^{-1} \approx 600\,\mathrm{MeV}$, where ρ_{av} denotes the average instanton size, the dynamics of the effective quark degrees of freedom is given by the partition function [76,77]

$$Z_{\mathrm{eff}} = \int \mathcal{D}\psi\,\mathcal{D}\bar\psi\mathcal{D}U\;\exp\left[i\,S_{\mathrm{eff}}(\bar\psi,\psi,U)\right],$$
$$S_{\mathrm{eff}}(\bar\psi,\psi,U) = \int \mathrm{d}^4x\;\bar\psi(i\partial\!\!\!/ - M\,U^{\gamma_5} - m)\psi. \qquad (13)$$

Here we restrict ourselves to two flavors and neglect isospin breaking effects with $m = m_u = m_d$ denoting the current quark mass, whereas $U = \exp(i\tau^a\pi^a)$ denotes the chiral pion field with $U^{\gamma_5} = \exp(i\gamma_5\tau^a\pi^a)$. The dynamical mass is, strictly speaking, momentum dependent, i.e., $M = M(p)$. However, in practical calculations it is convenient to work with a constant $M = M(0) = 350\,\mathrm{MeV}$ following from the instanton vacuum [75] and to regularize the effective theory by means of an explicit regularization with a cutoff of $\mathcal{O}(\rho_{\mathrm{av}}^{-1})$ whose precise value is fixed to reproduce the physical value of the pion decay constant $f_\pi = 93\,\mathrm{MeV}$. In this work we use the proper-time regularization.

The quark degrees of freedom of the effective theory (13) correspond to QCD quark degrees of freedom up to corrections that are small in the instanton packing fraction $\rho_{\mathrm{av}}/R_{\mathrm{av}} \sim \frac{1}{3}$, where R_{av} denotes the average separation of instantons. The same parameter suppresses the contribution of gluon degrees of freedom [74].

The CQSM is an application of the effective theory (13) to the description of baryons [42,43]. Although the Gaussian path integral over fermion fields in Eq. (13) can be solved exactly, the path integral over pion field configurations can be solved only in the large-N_c limit by means of the saddle-point approximation (in the Euclidean formulation of the theory). In the leading order of the large-N_c limit the pion field is static, and one can determine the spectrum of the one-particle Hamiltonian of the effective theory (13)

$$\hat H|n\rangle = E_n|n\rangle, \quad \hat H = -i\gamma^0\gamma^k\partial_k + \gamma^0 M U^{\gamma_5} + \gamma^0 m. \qquad (14)$$

The spectrum of Eq. (14) consists of an upper and a lower Dirac continuum, distorted by the pion field as compared to continua of the free Dirac-Hamiltonian $\hat H_0$ (given by $\hat H$ with U^{γ_5} replaced by 1), and of a discrete bound state level of energy E_{lev}, if the pion field is strong enough. By occupying the discrete level and the lower continuum states each by N_c quarks in an antisymmetric color state, one obtains a state with

unity baryon number. The soliton energy

$$E_{\rm sol}[U] = N_c \left[E_{\rm lev} + \sum_{E_n<0} (E_n - E_{n_0}) \right]_{\rm reg}. \qquad (15)$$

is a functional of the pion field. It is logarithmically divergent, see, e.g., Ref. [47] for explicit expressions in the proper-time regularization. By minimizing $E_{\rm sol}[U]$ one obtains the self-consistent solitonic pion field U_c. This procedure is performed for symmetry reasons in the so-called hedgehog ansatz $\pi^a(\mathbf{x}) = e_r^a\, P_c(r)$ with the radial (soliton profile) function $P_c(r)$ and $r = |\mathbf{x}|$, $\mathbf{e}_r = \mathbf{x}/r$. The nucleon mass M_N is given by $E_{\rm sol}[U_c]$.

In the large-N_c limit the path integral over U in Eq. (13) is solved by evaluating the expression at U_c and integrating over translational and rotational zero modes of the soliton solution. To include corrections in the $1/N_c$ expansion one considers time-dependent pion field fluctuations around the solitonic solution. In practice hereby one restricts oneself to time-dependent rotations of the soliton field in spin- and flavor-space that are slow because the corresponding soliton moment of inertia

$$I = \frac{N_c}{6} \sum_{\substack{m,\rm non\\ n,\rm occ}} \frac{\langle n|\tau^a|m\rangle\,\langle m|\tau^a|n\rangle}{E_m - E_n}\bigg|_{\rm reg} \qquad (16)$$

is large, $I = \mathcal{O}(N_c)$. It is logarithmically divergent and has to be regularized. In Eq. (16) one has to sum over occupied ("occ") states n that satisfy $E_n \leqslant E_{\rm lev}$, and over nonoccupied ("non") states m that satisfy $E_m > E_{\rm lev}$.

The model expressions for the nucleon EMT form factors in the effective theory (13) were derived explicitly in Ref. [60]. The gluon part of the EMT is zero in the effective theory (13), because there are no explicit gluon degrees of freedom. (So we omit the index Q when discussing the model results in this and in Secs. IV and V but restore it later.)

Consequently, in the model the quark part of the EMT is conserved by itself, and the form factor $\bar{c}(t)$ in Eq. (1) vanishes [60]. The model expressions for the other form factors read

$$M_2(t) - \frac{t}{5M_N^2} d_1(t) = \frac{1}{M_N} \int {\rm d}^3\mathbf{r}\; \rho_E(r)\; j_0(r\sqrt{-t}) \qquad (17)$$

$$d_1(t) = \frac{15 M_N}{2} \int {\rm d}^3\mathbf{r}\; p(r)\; \frac{j_0(r\sqrt{-t})}{t} \qquad (18)$$

$$J(t) = 3 \int {\rm d}^3\mathbf{r}\; \rho_J(r)\; \frac{j_1(r\sqrt{-t})}{r\sqrt{-t}}, \qquad (19)$$

with the Bessel functions $j_0(z) = \frac{\sin z}{z}$ and $j_1(z) = -j_0'(z)$. The Fourier transforms of the form factors, which are radial functions and to which we refer as "densities" in the following, are defined as

$$\rho_E(r) = N_c \sum_{n,\rm occ} E_n\; \phi_n^*(\mathbf{r})\phi_n(\mathbf{r})\,\big|_{\rm reg} \qquad (20)$$

$$p(r) = \frac{N_c}{3} \sum_{n,\rm occ} \phi_n^*(\mathbf{r})\,(\gamma^0 \boldsymbol{\gamma}\hat{\mathbf{p}})\,\phi_n(\mathbf{r})\,\big|_{\rm reg} \qquad (21)$$

$$\rho_J(r) = -\frac{N_c}{24 I} \sum_{\substack{n,\rm occ\\ j,\rm non}} \epsilon^{abc} r^a \phi_j^*(\mathbf{r})(2\hat{p}^b + (E_n + E_j)\gamma^0\gamma^b) \times \phi_n(\mathbf{r})\, \frac{\langle n|\tau^c|j\rangle}{E_j - E_n}\bigg|_{\rm reg}. \qquad (22)$$

The expressions in Eqs. (20), (21), and (22) are logarithmically UV divergent. Here we use the proper-time method to regularize them, see Refs. [60] for explicit expressions in this regularization. In Ref. [60] analytical proofs were given that

(i) the stability condition (11) is satisfied in the model,
(ii) the form factors satisfy the constraints at $t = 0$ in Eq. (8), and
(iii) the same expressions for EMT form factors follow in the model from unpolarized GPDs via the sum rules (2).

Notice that the latter is a special case of the "polynomiality property" of GPDs [17] satisfied in the CQSM [56,57]. The field-theoretic character of the model is a crucial prerequisite that allows formulation and analytical proofs of such and other [49] general QCD requirements. This in turn provides important cross-checks for the theoretical consistency of the approach.

For the numerical calculation we employ the so-called Kahana-Ripka method [78], whose application to calculations of the nucleon EMT form factors in the CQSM is briefly described in Ref. [60]. The use of the proper-time regularization has the advantage (over, e.g., the Pauli-Villars method [79]) that it is possible to include explicitly chiral symmetry breaking effects due to a finite current quark mass m in the effective action (13).

In Ref. [41] it was shown that it is possible to obtain soliton solutions and compute nucleon masses for current quark masses up to $m = \mathcal{O}(700\,{\rm MeV})$ that correspond to pion masses up to $m_\pi = \mathcal{O}(1.5\,{\rm GeV})$. What provides a certain justification for the application of the model up such large m is the fact that the model *formally* contains the correct heavy quark limit result for the nucleon mass [41]. The proof that in the limit $m \to m_Q$, where m_Q is the heavy quark mass, the nucleon mass tends to $M_N \to N_c m_Q$ given in Ref. [41] is *formal* because in this proof it was taken for granted that stable soliton solutions do exist up to such large pion mass values.

Therefore, it was of importance in Ref. [41] to demonstrate numerically the existence of soliton solutions for large m_π up to, at least, $m_\pi = \mathcal{O}(1.5\,{\rm GeV})$. These soliton solutions were found by using a standard iteration procedure for the calculation of the self-consistent profile function $P_c(r)$ described in detail, e.g., in Ref. [47]. Here, as a by-product of our study of EMT form factors, we will be in the position to provide an important and valuable cross-check. Namely do the pressures $p(r)$ computed with the respective large-m_π soliton profiles really satisfy the stability condition (11)? The answer is yes; see below Sec. IV D.

Before discussing the m_π dependence of the densities (20), (21), and (22) and the form factors (17), (18), (19) we have to establish which model parameters are allowed to vary and which are kept fixed while m_π is varied. Here we shall use the choice of Ref. [41] to keep $M = 350\,{\rm MeV}$ and $f_\pi = 93\,{\rm MeV}$

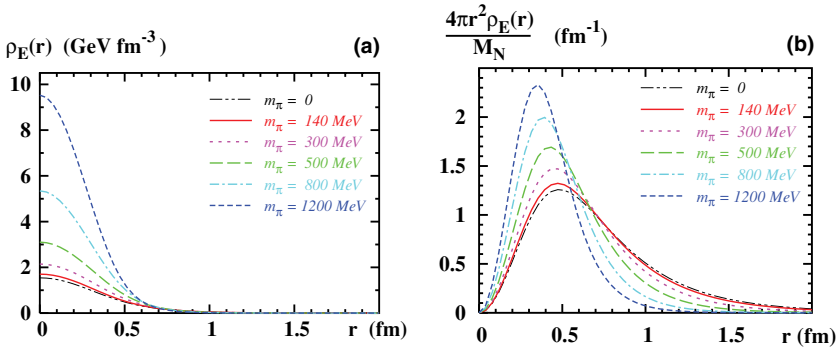

FIG. 1. (Color online) (a) The energy density $\rho_E(r)$ of the nucleon as function of r for different pion masses. (b) The normalized energy density $4\pi r^2\rho_E(r)/M_N$ as function of r for different pion masses. The curves are normalized such that one obtains unity upon integration over r.

fixed. Then the proper-time cutoff is adjusted such that for a given m and m_π one reproduces the physical value of f_π (m and m_π are related to each other in the effective theory (13) by a relation which for small m corresponds to the Gell-Mann—Oakes—Renner relation; see Ref. [41]).

This way of parameter handling in the model was found to provide a good description of lattice data on the variation of $M_N(m_\pi)$ with m_π, once one takes into account the generic overestimate of the nucleon mass in the soliton approach [80]. However, the above way of parameter handling is just one possible choice and other choices are possible as well. An investigation whether other choices of parameter handling yield equally satisfactory results will be presented elsewhere.

IV. THE DENSITIES OF THE EMT

In this section we focus our attention on the densities (20), (21), and (22), which are interesting objects by themselves, before we discuss the form factors (17), (18), and (19) in the next section. The study of the densities will enable us to address the question whether the model provides a satisfactory description of the nucleon in (fictious) worlds with pion masses up to 1.2 GeV. As we shall see, the answer is yes.

A. Energy density

The energy density $\rho_E(r)$ is just $T^{00}(r)$ in the static EMT (3) and is normalized as $\int d^3\mathbf{r}\,\rho_E(r, m_\pi) = M_N(m_\pi)$ for any m_π where we explicitly indicate the pion mass dependence. $M_N(m_\pi)$ as function of m_π was studied in Ref. [41].

Figure 1(a) shows $\rho_E(r)$ as function of r for pion masses in the range $0 \leqslant m_\pi \leqslant 1.2$ GeV. In the following we focus on the region $m_\pi \geqslant 140$ MeV, and include only for completeness the results for $m_\pi \leqslant 140$ MeV discussed in detail in Ref. [60].

In the physical situation with $m_\pi = 140$ MeV the energy density in the center of the nucleon is $1.7\,\mathrm{GeV\,fm^{-3}}$ or $3.0 \times 10^{15}\,\mathrm{g\,cm^{-3}}$. This corresponds roughly to 13 times the equilibrium density of nuclear matter. As m_π increases $\rho_E(0)$ becomes larger and reaches $\rho_E(0) = 9.5\,\mathrm{GeV\,fm^{-3}} = 17 \times 10^{15}\,\mathrm{g\,cm^{-3}}$ at $m_\pi = 1.2$ GeV. At the same time, with increasing m_π the fall-off of $\rho_E(r)$ at large r becomes stronger, as can be seen in Fig. 1(b).

These observations mean that with increasing m_π the nucleon becomes "smaller." To quantify this statement we consider the mean square radius of the energy density defined as

$$\langle r_E^2\rangle = \frac{\int d^3\mathbf{r}\, r^2\rho_E(r)}{\int d^3\mathbf{r}\,\rho_E(r)}\,, \tag{23}$$

which decreases with increasing m_π. The pion mass dependence of $\rho_E(0)$ is shown in Fig. 2(a), see also Table I where many results are summarized. We observe an approximately linear growth of $\rho_E(0)$ with m_π^2. The pion mass dependence of $\langle r_E^2\rangle$ is shown in Fig. 2(b), see also Table I. Up to $m_\pi \lesssim 400$ MeV we observe a roughly linear decrease of $\langle r_E^2\rangle$ with m_π which proceeds at a slower rate for $m_\pi \gtrsim 400$ MeV. (Throughout we choose a linear or quadratic in m_π presentation of the m_π dependence of the quantities—depending on which one is more convenient.)

The above observations can be intuitively understood. With increasing m_π the range of the "pion cloud" decreases. This results in a less wide spread nucleon. The above observations are also consistent with what one expects from the heavy quark limit point of view. The heavier the constituents building up a

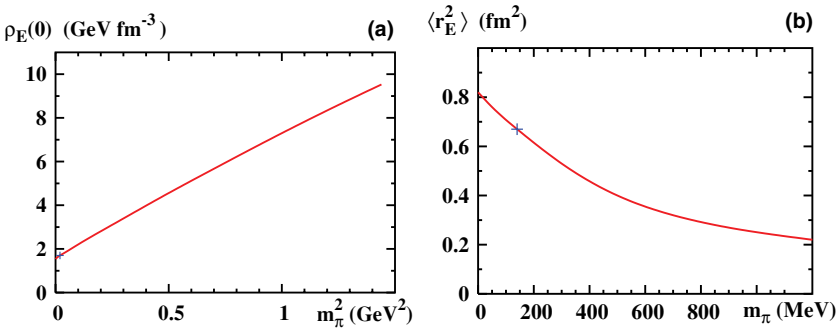

FIG. 2. (Color online) The pion mass dependence of (a) the energy density $\rho_E(0)$ in the center of the nucleon, and (b) the mean square radius of the energy density $\langle r_E^2\rangle$ defined in Eq. (23). The crosses indicate the physical point.

TABLE I. The pion mass dependence of different quantities computed in the CQSM using proper time regularization: the energy density in the center of the nucleon $\rho_E(0)$, the mean square radii $\langle r_E^2\rangle$ and $\langle r_J^2\rangle$, the pressure $p(0)$ in the center of the nucleon, the position r_0 of the zero of the pressure defined as $p(r_0)=0$, the constant d_1, the dipole masses of the form factors $M_2(t)$, $J(t)$, and $d_1(t)$, and the mean square radius $\langle r_F^2\rangle$ of the trace of the EMT operator. In the chiral limit $J(t)$ and $d_1(t)$ have infinitely steep slopes at $t=0$, see text. In these cases dipole fits do not provide useful approximations and are undefined (labeled "undef." in the table). The results for $m_\pi \leqslant 140$ MeV from Ref. [60] are included for completeness.

m_π (MeV)	$\rho_E(0)$ (GeV/fm^3)	$\langle r_E^2\rangle$ (fm^2)	$\langle r_J^2\rangle$ (fm^2)	$p(0)$ (GeV/fm^3)	r_0 (fm)	d_1	Dipole masses $M_{\rm dip}$ in GeV for			$\langle r_F^2\rangle$ (fm^2)
							$M_2(t)$	$J(t)$	$d_1(t)$	
0	1.54	0.82	∞	0.195	0.59	−3.46	0.867	Undef.	Undef.	1.04
50	1.57	0.76	1.88	0.202	0.59	−3.01	0.873	0.692	0.519	0.95
140	1.70	0.67	1.55	0.232	0.57	−2.35	0.906	0.745	0.646	0.81
300	2.14	0.53	1.11	0.298	0.54	−1.81	0.990	0.844	0.872	0.62
500	3.10	0.40	0.77	0.377	0.51	−1.66	1.111	0.986	1.069	0.46
700	4.50	0.32	0.59	0.450	0.49	−1.60	1.228	1.120	1.214	0.37
900	6.86	0.26	0.48	0.553	0.46	−1.55	1.334	1.237	1.337	0.29
1200	9.53	0.22	0.38	0.597	0.42	−1.47	1.473	1.390	1.492	0.24

hadron, the smaller is the size of that hadron. Thus, the model results for $\rho_E(r)$ are in agreement with what one expects for increasing m_π.

We remark that, being a chiral model, the CQSM correctly describes the behavior of $\langle r_E^2\rangle$ in the chiral limit [60].

B. Angular-momentum density

The angular-momentum density $\rho_J(r)$ is related to the T^{0k} components of the static EMT as $\rho_J(r)=\epsilon^{ijk}s_i x_j T_{0k}(\mathbf{x})$. Figure 3(a) shows $\rho_J(r)$ as function of r for different pion masses. For any m_π we find that $\rho_J(r)\propto r^2$ at small r, it reaches then a maximum around $r\simeq(0.3-0.4)$ fm and goes slowly to zero at large r.

As m_π increases we observe that the density $\rho_J(r)$ becomes larger in the small r region at the price of decreasing in the region of larger r. The increase in one and decrease in another region of r (as m_π is varied) occurs in a precisely balanced way, because $\rho_J(r)$—in contrast to the energy density—is always normalized as $\int d^3\mathbf{r}\,\rho_J(r,m_\pi)=J_N=\frac{1}{2}$, independently of m_π. These observations can be understood within the picture of a rigidly rotating soliton as follows. For large pion masses the "matter" inside the soliton is localized more toward its center, as we have observed above, such that the inner region of the soliton plays a more important role for its rotation. As m_π decreases, and hence the range of the pion cloud increases, the energy density in the soliton becomes more strongly delocalized, and then the "outer regions" play a more and more important role for the rotation of the soliton.

These findings can be quantified by considering the mean square radius $\langle r_J^2\rangle$ of the angular momentum density defined analogously to Eq. (23). Figure 3(b) shows $\langle r_J^2\rangle$ as function of m_π, and we see that $\langle r_J^2\rangle$ decreases with increasing m_π. Notice that in the chiral limit $\rho_J(r)\propto 1/r^4$ at large r such that $\langle r_J^2\rangle$ diverges [60]. Our numerical results for $\langle r_J^2\rangle$ in Fig. 3(b) indicate this effect.

C. Pressure and shear forces

Next we turn to the discussion of the distributions of pressure and shear forces, $p(r)$ and $s(r)$, which are related to the T^{ik} components of the static EMT.

Figures 4(a) and 4(b) show the distributions of pressure $p(r)$ and shear forces $s(r)$ as functions of r for different m_π. For all m_π the distributions of pressure and shear forces exhibit the same qualitative behavior. The pressure takes at $r=0$ its global maximum, decreases monotonically becoming zero at some point r_0 until it reaches its global minimum at some point, $r_{p,\,\rm min}$, and decreases, monotonically tending to zero but always remaining negative. The distribution of shear forces is never negative. It starts at a zero value at $r=0$, increases monotonically until it reaches a global maximum at some point, $r_{s,\rm max}$, and decreases then monotonically tending to zero.

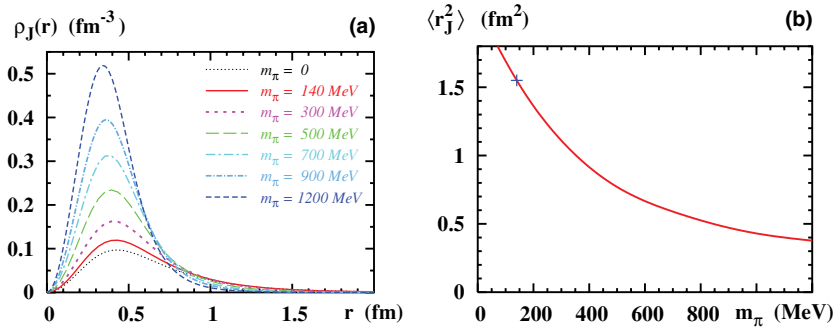

FIG. 3. (Color online) (a) The angular momentum density $\rho_J(r)$ as function of r for different pion masses m_π. (b) The mean square radius $\langle r_J^2\rangle$ of the angular momentum density as function of m_π.

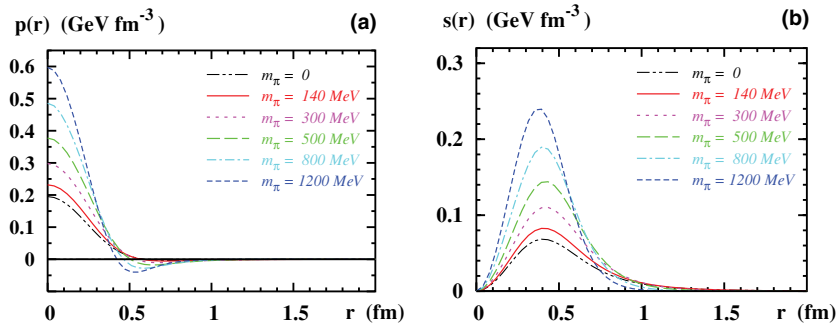

FIG. 4. (Color online) The distributions of (a) pressure $p(r)$ and (b) the shear forces $s(r)$ as functions of r for different pion masses.

The positive sign of the pressure for $r < r_0$ corresponds to repulsion, whereas the negative sign in the region $r > r_0$ means attraction. This is intuitive because in the inner region we expect repulsion among quarks due to the Pauli principle, whereas the attraction in the outer region is an effect of the pion cloud which is responsible for binding the quarks to form a nucleon [60].

With increasing m_π the pressure $p(0)$ in the center of the nucleon increases. At the same time also the absolute value of its (negative) minimum increases. Also the maximum of $s(r)$ becomes larger with increasing m_π, whereas the characteristic positions r_0, $r_{p,\,\mathrm{min}}$, and $r_{s,\,\mathrm{max}}$ move toward smaller r, see Fig. 5 for m_π dependence of $p(0)$ and r_0.

These observations can be understood as follows. The repulsive forces in the center of the nucleon increase as a response to the higher density at larger m_π. At the same time the size of the nucleon decreases requiring stronger binding forces—and a "movement" of characteristic length scales of $p(r)$ and $s(r)$ toward the center. At any m_π repulsive and attractive forces are precisely balanced due to Eq. (11); see Sec. IV D.

D. Stability

Although the densities, $\rho_E(r)$ and $\rho_J(r)$, are normalized with respect to M_N and J_N, for the pressure $p(r)$ the corresponding analogon is the stability criterion (11). In Ref. [60] it was proven analytically that Eq. (11) is satisfied in the model—provided one evaluates the pressure with the self-consistent profile, i.e., with that profile which for a given m_π provides the true minimum of the soliton energy (15).

For given model parameters the soliton profiles are obtained by means of an iteration procedure that is described in detail in, for example, Ref. [47]. The profiles used here were computed in Ref. [41] where a good convergence of the iteration procedure was observed. However, what precisely means that the convergence of the iteration was good? In other words, how to test the quality of the numerical results? One could, for example, slightly modify the obtained profiles and check that they yield larger soliton masses than the respective true self-consistent profile. But the probably most elegant method is provided by the stability criterion (11). If, and only if, we found the soliton profile that truly minimizes the soliton energy (11), the pressure computed with that profile will satisfy (11).

One way to check to which numerical accuracy our results satisfy Eq. (11) is as follows. Let us consider $r^2 p(r)$ as function of r, see Fig. 6(a), and compute the integrals from 0 to r_0 and from r_0 to ∞.[1] We obtain

$$\int_0^{r_0} \mathrm{d}r\; r^2 p(r) = \begin{cases} 2.614\ \mathrm{MeV} \\ 3.737\ \mathrm{MeV} \\ 3.856\ \mathrm{MeV}, \end{cases}$$

$$\int_{r_0}^{\infty} \mathrm{d}r\; r^2 p(r) = \begin{cases} -2.630\,\mathrm{MeV} \\ -3.748\,\mathrm{MeV} \\ -3.861\,\mathrm{MeV}, \end{cases}$$

[1]The numerical calculations are carried carried out in a finite spherical volume—here of the size $D = 12$ fm. For most quantities the densities decay fast enough at large r such that it is sufficient to integrate up to $r = D$. This is what we did in Eq. (24). However, for certain quantities given by integrals over the densities weighted by a higher power of r the integrands may happen not to be negligibly small at large r in particular for small $m_\pi \lesssim 140$ MeV. Then it is necessary to explore the analytically known large-r asymptotics of the densities, see Ref. [60], and to include the contribution of the regions $r > D$ not covered in the numerical calculation. Examples of such quantities are d_1 or $\langle r_J^2 \rangle$. The latter is divergent in the chiral limit, see Sec. IV B.

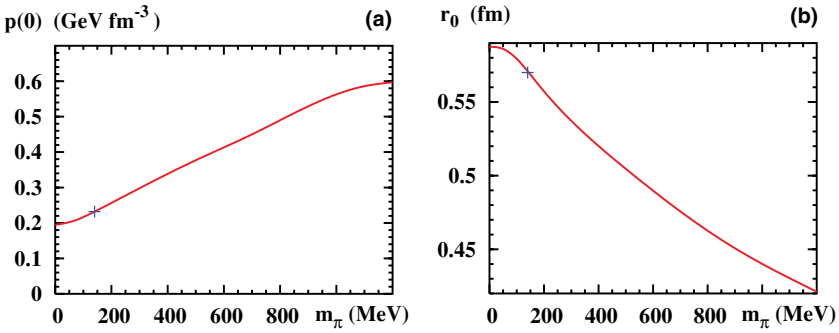

FIG. 5. (Color online) The pion mass dependence of the pressure $p(0)$ in the center of the nucleon and of the position r_0 at which $p(r)$ vanishes.

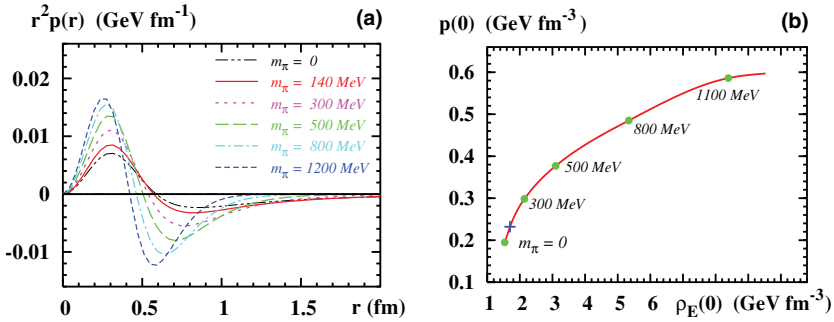

FIG. 6. (Color online) (a) $r^2\,p(r)$ as function of r for different pion masses. The integrals over the regions where $r^2\,p(r)$ is, respectively, positive and negative cancel each other within numerical accuracy of better than 1%. This shows how the stability condition in Eq. (11) is satisfied; see text. (b) The pressure $p(0)$ as function of the energy density $\rho_E(0)$ in the center of the nucleon. Some pion masses to which the respective values refer are indicated. The physical point is marked by the cross.

$$\text{i.e.,}\ \frac{\left|\int_0^\infty \mathrm{d}r\ r^2\,p(r)\right|}{\int_0^\infty \mathrm{d}r\ r^2|p(r)|} = \begin{cases} 0.31\% & \text{for}\ \ m_\pi = 140\,\text{MeV} \\ 0.15\% & \text{for}\ \ m_\pi = 500\,\text{MeV} \\ 0.07\% & \text{for}\ \ m_\pi = 1200\,\text{MeV}, \end{cases} \tag{24}$$

and see that the stability criterion is satisfied to within a satisfactory numerical accuracy. Finally, we may test another sort of stability. We may ask the question how do pressure and energy density in the center of nucleon depend on each other for varying m_π. In fact, with $\rho_E(r, m_\pi)$ and $p(r, m_\pi)$ at hand, we may eliminate m_π at $r = 0$ and express $p(0)$ as function of $\rho_E(0)$. This is shown in Fig. 6(b) which demonstrates how the center of the nucleon responds to changes of m_π. Understanding the center of the nucleon for a moment as a "medium which is subject to variations of the external parameter m_π" we observe that for any m_π we have $\frac{\partial p(\rho_E)}{\partial \rho_E} > 0$. This is a criterion for stability of a system that must respond with an increase of pressure if the density is increased.

V. RESULTS FOR THE FORM FACTORS

Figure 7 shows the form factors of the EMT as functions of t for $|t| \leqslant 1\,\text{GeV}^2$ for different m_π. All EMT form factors (with the exception of $J(t)$ and $d_1(t)$ in the chiral limit, see below) can be well approximated by dipole fits of the kind

$$F(t) = \frac{F(0)}{\left(1 - t/M_{\text{dip}}^2\right)^2}. \tag{25}$$

It is instructive to compare within the model the EMT form factors to the electromagnetic form factors—for example, to the electric form factor of the proton $G_E(t)$ [46]. Interestingly, $J(t)$ and $G_E(t)$ show a similar t dependence. But $M_2(t)$ falls off with increasing $|t|$ slower than $G_E(t)$, whereas $d_1(t)$ exhibits a faster fall off, see Ref. [60] for more details.

The dipole masses of the different form factors exhibit different m_π dependences, see Fig. 8(a) and Table I. For all form factors the dipole masses increase with increasing m_π. It is an interesting observation that the dipole masses of $M_2(t)$ and $J(t)$ exhibit for $m_\pi \gtrsim 140\,\text{MeV}$ to a good approximation a linear dependence on m_π. But the m_π dependence of the dipole mass of $d_1(t)$ follows a different pattern. We shall comment more on that in Sec. VII.

That the dipole approximation for $J(t)$ and $d_1(t)$ fails in the chiral limit, is due to fact that the slopes of $J(t)$ and $d_1(t)$ at $t = 0$ diverge in this limit [60]. For $J(t)$ this is clear because its derivative at $t = 0$ is related to the mean square radius of the angular momentum density as $J'(0) = \frac{1}{6}\langle r_J^2\rangle$, and $\langle r_J^2\rangle$ diverges for $m_\pi \to 0$, see Sec. IV B.

The slope of $d_1(t)$ at $t = 0$ becomes infinitely steep in the chiral limit because it is related as $d_1'(0) = \frac{M_N}{16}\int \mathrm{d}^3\mathbf{r}\ r^4\,p(r)$ to the pressure that behaves as $p(r) \propto \frac{1}{r^6}$ at large r in the chiral limit. More precisely, $d_1'(t) \propto 1/\sqrt{-t}$ at small t in the chiral limit. For small but nonzero m_π the derivative $d_1'(0)$ exists and is proportional to $1/m_\pi$. These results hold both in the CQSM [60] and in χPT [31]. The derivative of the form factor $M_2(t)$ at $t = 0$ is finite for any m_π.

$M_2(t)$ and $J(t)$ are normalized at $t = 0$ for any m_π as $M_2(0) = 2J(0) = 1$ [60]. In the CQSM these constraints are

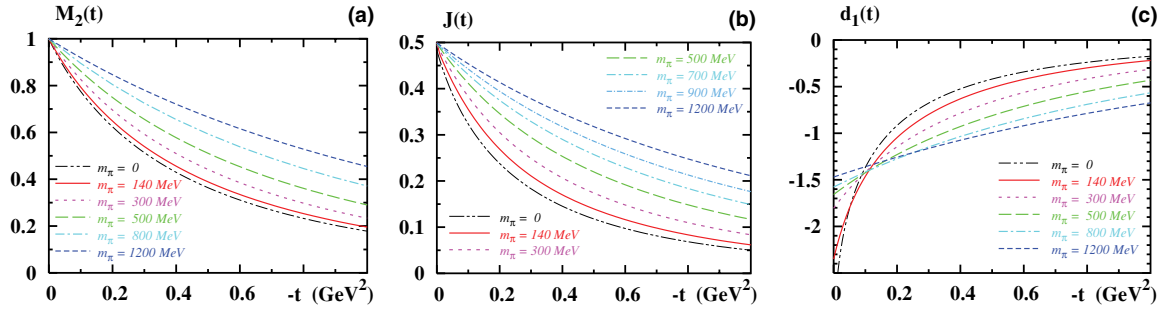

FIG. 7. (Color online) The form factors of the energy momentum tensor $M_2(t)$, $J(t)$, and $d_1(t)$ as functions of t for different pion masses. In the chiral limit $J(t)$ and $d_1(t)$ exhibit infinitely steep slopes at $t = 0$, and $d_1(0)$ takes the value -3.46, which does not fit on the scale in Fig. 7(c).

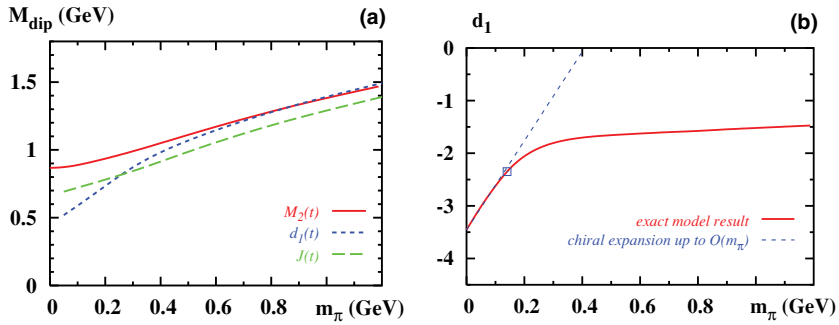

FIG. 8. (Color online) (a) The dipole masses as defined in Eq. (25) for the form factors $M_2(t)$, $d_1(t)$, and $J(t)$ from the CQSM vs. m_π. Notice that $d_1(t)$ and $J(t)$ cannot be approximated by dipoles for $m_\pi = 0$. (b) The constant d_1 as function of m_π at low scale. (Solid line) The exact result from the CQSM. (Dotted line) The chiral expansion of $d_1(m_\pi)$ to linear order in m_π according to (26). The square marks the physical point.

consistent for they mean that entire momentum and spin of the nucleon are carried by quark degrees of freedom. The numerical results satisfy these constraints within a numerical accuracy of better than 1%; see Figs. 7(a) and 7(b).

In contrast, no principle fixes the normalization of the form factor $d_1(t)$ at $t = 0$ neither in the model nor in QCD. For all m_π we find $d_1 = d_1(0) < 0$. This condition has been conjectured to be dictated by stability requirements [60]. Figure 8(b) shows the m_π dependence of d_1, which is rather strong. This is due to the fact that d_1 receives a large leading nonanalytic contribution proportional to m_π. (The "nonanalyticity" refers to the current quark mass $m \propto m_\pi^2$.) The chiral expansion of d_1 reads

$$d_1(m_\pi) = \overset{\circ}{d}_1 + k\,\frac{5\,g_A^2 M_N}{64\,\pi\,f_\pi^2}\,m_\pi + \ldots \tag{26}$$

where $\overset{\circ}{d}_1$ denotes the chiral limit value of d_1, and the dots indicate subleading terms in the chiral limit. Because the limits $N_c \to \infty$ and $m_\pi \to 0$ do not commute [81,82] one has in Eq. (26) $k = 1$ for finite N_c [31] and $k = 3$ in the large-N_c limit [60]. The latter corresponds to the situation in the CQSM.

It is interesting to observe that the leading nonanalytic term in the chiral expansion of d_1 in Eq. (26) dominates the chiral behavior of d_1 up to the physical point, see Fig. 8(b). But for larger m_π higher orders in the chiral expansion become important, and change the qualitative m_π-behavior of $d_1(m_\pi)$. We shall come back to this point in Sec. VII.

Finally, we discuss m_π dependence of the mean square radius $\langle r_F^2\rangle$ of the trace of the total EMT operator given due to the trace anomaly [83] by

$$\hat{T}^\mu_\mu \equiv \frac{\beta}{2g}\,F^{\mu\nu}F_{\mu\nu} + (1+\gamma_m)\sum_a m_a\bar{\psi}_a\psi_a. \tag{27}$$

Let $F(t)$ denote the form factor of the operator (27) which is normalized as $F(0) = 1$. Its slope at $t = 0$ defines $\langle r_F^2\rangle = 6F'(0)$ which can be related as

$$\langle r_F^2\rangle = \langle r_E^2\rangle - \frac{12\,d_1}{5M_N^2} \tag{28}$$

to $\langle r_E^2\rangle$ and d_1, see Ref. [60]. Figure 9 shows how $\langle r_F^2\rangle$ depends on the pion mass. In the chiral limit $\langle r_F^2\rangle$ is the mean square radius of the operator $F^{\mu\nu}F_{\mu\nu}$ and its large value there is in contrast to what is known about the mean square radii of other gluonic operators [84].

VI. COMPARISON TO LATTICE RESULTS

It is instructive to compare the results for the form factors of the EMT to lattice QCD data [24–28]. Presently, this offers actually the only available test for the model results. For the comparison it is necessary to evolve the model results from a low initial scale $\mu_0 \sim 0.6\,\text{GeV}$ to typically $\mu \sim 2\,\text{GeV}$ in the lattice calculations which we shall do to leading logarithmic accuracy. Under evolution the quark (flavor-singlet) form factors mix with the corresponding gluon form factors. We set the latter to zero at the initial scale.

In this context it is worthwhile recalling that in early parametrizations of unpolarized parton distributions $f_1^a(x)$, the gluon (and sea quark) distribution(s) and thus M_2^G were assumed to be zero at a low initial scale [85]. One success of these approaches was that they were able to explain the observation $M_2^Q \approx 0.5$ at $\mu^2 \sim 5\,\text{GeV}^2$. That is, starting with $M_2^Q = 1$ and $M_2^G = 0$ at a low scale, which is the situation in the CQSM, it is possible to reproduce the observation $M_2^Q \approx 0.5$ at several GeV^2. However, with the advent of more data (especially at low x) it became clear [86] that nonzero gluon (and see quark) distributions are required already at low initial scales. Modern parametrizations performed at low scales require a sizable gluon distribution and $M_2^G \approx 0.3$ [87]. This is not in disagreement with the instanton picture where twist-2 gluon operators are suppressed with respect to quark operators by the instanton packing fraction which is numerically of order 30% [74]. Thus in some sense the phenomenologically required "portion of gluons" is within the accuracy of the model [51]. With these remarks in mind we conclude that the CQSM result $M_2^Q = 1$ at the low scale of the model is in agreement with phenomenology—within the

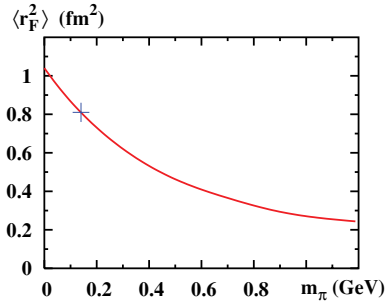

FIG. 9. (Color online) The mean square radius $\langle r_F^2\rangle$ of the trace of the total EMT operator vs. m_π.

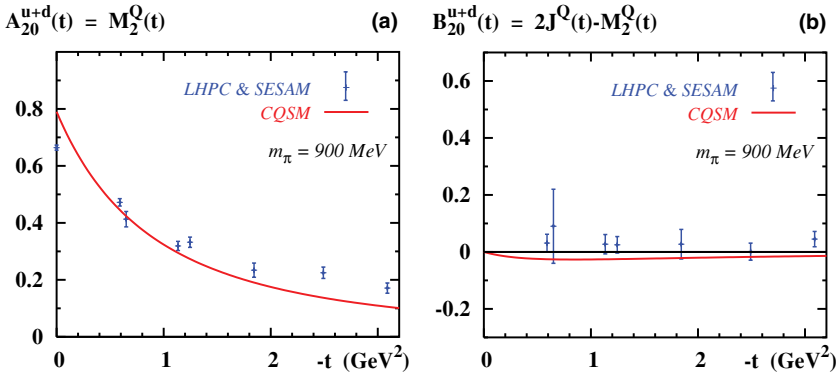

FIG. 10. (Color online) The form factors of the energy momentum tensor $A_{20}^{u+d}(t) \equiv A^Q(t) = M_2^Q(t)$ and $B_{20}^{u+d}(t) \equiv B^Q(t) = 2J^Q(t) - M_2^Q(t)$ as functions of t at the scale $\mu = 2\,\mathrm{GeV}$ in a world with pion mass $m_\pi = 900\,\mathrm{GeV}$. (See Appendix for the discussion of different notations.) The lattice data points are by the LHPC and SESAM Collaborations [26]. The solid curves are the results from the CQSM obtained here.

accuracy of this model. Next, before we compare the results from the model to those from lattice QCD, let us confront the lattice results [24–28] with predictions from the large-N_c limit. In this limit one has for $|t| \ll M_N^2$ independently of the scale [19]

$$\begin{aligned} \underbrace{(A^u + A^d)(t)}_{\mathcal{O}(N_c^0)} &\gg \underbrace{|(A^u - A^d)(t)|}_{\mathcal{O}(N_c^{-1})}\,, \\ \underbrace{|(B^u - B^d)(t)|}_{\mathcal{O}(N_c)} &\gg \underbrace{|(B^u + B^d)(t)|}_{\mathcal{O}(N_c^0)}, \\ \underbrace{|(C^u + C^d)(t)|}_{\mathcal{O}(N_c^2)} &\gg \underbrace{|(C^u - C^d)(t)|}_{\mathcal{O}(N_c)}, \end{aligned} \tag{29}$$

cf. Appendix for the explanation of the notation. For completeness let us quote that the gluon form factors satisfy

$$A^G(t) = \mathcal{O}\big(N_c^0\big), \quad B^G(t) = \mathcal{O}\big(N_c^0\big), \quad C^G(t) = \mathcal{O}\big(N_c^2\big), \tag{30}$$

which is the same large-N_c behavior as the corresponding quark-flavour-singlet form factors.

Remarkably, although in the real world $N_c = 3$ does not seem to be large, nevertheless lattice data [24–28] reflect the large-N_c flavor dependence of the quark form factors (29). In fact, large-N_c relations of the type (29), (30) are observed to be satisfied in phenomenology [88] and serve within their range of applicability as useful guidelines [89]. The soliton approach is justified in the large-N_c limit [44] and satisfies general large-N_c relations of the type (29). The observation that the lattice results [24–28] are compatible with (29) is therefore an encouraging prerequisite for our study.

Let us first compare the model results to the lattice data computed by the LHPC and SESAM Collaborations [26]. There unquenched SESAM Wilson configurations on a $16^3 \times 32$ lattice at $\beta = 5.6$ with $\kappa = 0.1560$ were used. This corresponds to $m_\pi = (896 \pm 6)\,\mathrm{MeV}$ and a lattice spacing of $a = 0.098\,\mathrm{fm}$ with physical units fixed by extrapolating the nucleon mass. The form factor $A_{20}^{u+d}(t) = A^Q(t) \equiv M_2^Q(t)$ was computed omitting disconnected diagrams at a scale $\mu = 2\,\mathrm{GeV}$ for $0 \leqslant |t| \leqslant 3.1\,\mathrm{GeV}^2$. (The different notations are discussed in Appendix) The lattice data for $A^Q(t)$, which can be fit to the dipole form, are shown in Fig. 10(a). In Fig. 10(a) we also show the CQSM results evolved to the same scale for $|t| \lesssim 1\,\mathrm{GeV}^2$. We observe that the model results agree with the lattice data [26] to within 15% which is within the accuracy to which the CQSM results typically agree with phenomenology.

Figure 10(b) shows the form factor $B_{20}^{u+d}(t) = B^Q(t) \equiv 2J^Q(t) - M_2^Q(t)$ from Ref. [26] which was computed in the range $-t \in [0.59, 3.1]\,\mathrm{GeV}$ and was found consistent with zero within the statistical accuracy of the simulation. Also in the CQSM we find $B^Q(t)$ close to zero—in reasonable agreement with the lattice data; see Fig. 10(b). Notice that in the model, at the low scale, we have $B^Q(0) = 0$ because $M_2^Q(0) = 2J^Q(0)$ (and equal unity); see Secs. IV A and IV B. This implies a vanishing quark contribution to the "gravitomagnetic moment" of the nucleon [58] conjectured in Ref. [90]. The smallness of $B^Q(t)$ implies that to a good approximation $2J^Q(t) \approx M_2^Q(t)$. We come back to this point below.

Next, let us compare to the quenched lattice results by the QCDSF Collaboration [27], which were obtained using nonperturbatively $\mathcal{O}(a)$ improved Wilson fermions on a $16^3 \times 32$ lattice at $\beta = 6.0$ using varying values of κ. In Figs. 11(a), 11(b), and 11(c) the form factors $A_2^{u+d}(t) = A^Q(t) \equiv M_2^Q(t)$ and $B_2^{u+d}(t) = B^Q(t) \equiv 2J^Q(t) - M_2^Q(t)$ and $C_2^{u+d}(t) = C^Q(t) \equiv \frac{1}{5}d_1(t)$ are shown for $m_\pi = 640\,\mathrm{MeV}$ [27]. The results refer to a scale of $\mu = 2\,\mathrm{GeV}$ and cover the regions $-t \in [0, 2.8]\,\mathrm{GeV}^2$ for $A^Q(t)$ and $[0.6, 2.8]\,\mathrm{GeV}^2$ for $B^Q(t)$ and $C^Q(t)$. For comparison we plot the CQSM results at the corresponding scale and value of m_π. Also here we observe a satisfactory agreement with the lattice data within model accuracy and/or within the statistical accuracy of the lattice data.

Notice that the presence of explicit kinematical factors of $\mathcal{O}(\Delta)$ in the case of $B^Q(t)$, and of $\mathcal{O}(\Delta^2)$ in the case of $C^Q(t)$, see Eq. (A1) in App. A, practically amplifies the statistical errors of the form factors—as can be seen in Figs. 10 and 11. This is also the reason why no results for $C^Q(t)$ were presented in the exploratory study of Ref. [26].

The value of $2J^Q(t) \equiv (A^Q + B^Q)(t)$ at $t = 0$ is of particular interest since it gives the percentage of the total nucleon spin carried by quarks [5]. The lattice calculations yield

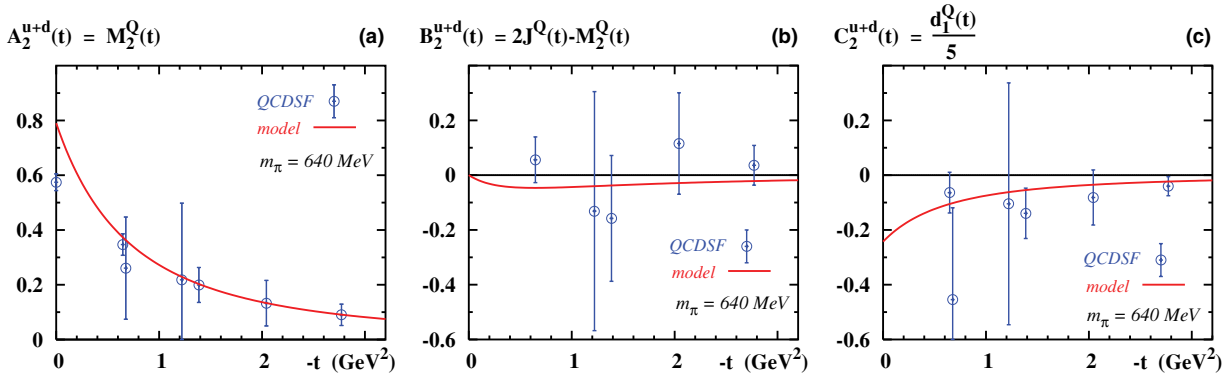

FIG. 11. (Color online) The form factors of the energy momentum tensor $A_2^{u+d}(t) \equiv A^Q(t) = M_2^Q(t)$ and $B_2^{u+d}(t) \equiv B^Q(t) = 2J^Q(t) - M_2^Q(t)$ and $C_2^{u+d}(t) \equiv C^Q(t) = \frac{1}{5}d_1^Q(t)$ as functions of t at the scale $\mu = 2$ GeV in a world with pion mass $m_\pi = 640$ GeV. (For notations see Appendix.) The lattice data points are from the QCDSF Collaboration [27]. The solid curves are the results from the CQSM obtained here.

$$2J^Q(0) = \begin{cases} 0.60 \pm 0.07 & \text{at} \quad \mu = 1.76 \text{ GeV extrapolated to the physical point [24]} \\ 0.70 \pm 0.20 & \text{at} \quad \mu \sim 1.8 \text{ GeV for } m_\pi \sim 0.8 \text{ GeV [25]} \\ 0.66 \pm 0.07 & \text{at} \quad \mu = 2 \text{ GeV extrapolated to the physical point [27]} \\ 0.682 \pm 0.018 & \text{at} \quad \mu = 2 \text{ GeV for } m_\pi = 900 \text{ MeV [26]}. \end{cases} \tag{31}$$

In the CQSM we have $2J^Q(0) = 1$ for any m_π at the low scale of the model, because there are only quarks and antiquarks to carry the nucleon angular momentum, and they must, of course, carry 100% of it. Considering evolution one obtains

$$2J^Q(0) \approx 0.75 \quad \text{from CQSM at} \quad \mu \approx (1.7 - 2.0)\,\text{GeV}, \tag{32}$$

and $2J^G(0) \approx 0.25$. The result [Eq. (32)] is—within model accuracy—in good agreement with the lattice data in Eq. (31).

For other aspects in the context of the nucleon spin structure discussed from the CQSM point of view the reader is referred to Ref. [59].

VII. CHIRAL EXTRAPOLATION OF LATTICE DATA

Let us draw from our study some conclusions which could be of interest in the context of the chiral extrapolation of lattice data. Unfortunately, the model cannot provide any insights in this respect concerning the m_π dependence of M_2^Q or J^Q. At the low scale $M_2^Q = 2J^Q = 1$ which expresses consistently that the total nucleon momentum and angular momentum in the model are carried by quarks—irrespective the value of m_π. The model provides, however, interesting results for the t dependence of $M_2^Q(t)$, $J^Q(t)$, and $d_1^Q(t)$, including the normalization of the latter.

For that let us imagine that for some reason we were able to compute in the CQSM the EMT form factors only for $m_\pi \gtrsim$ (400–500) MeV, and then forced to extrapolate the results down to small m_π to compare to the real world—using the model results from the large-m_π region as main guideline. What would we obtain?

First of all we emphasize that in the CQSM all form factors of the EMT can be well approximated by dipoles. Though there is some prejudice in this respect based on the experience with the electric and magnetic form factors of the proton, this is an important and nontrivial observation.

Next, we consider the dipole masses of the form factors $M_2^Q(t)$ and $J^Q(t)$. From the approximately linear m_π-behavior of the respective dipole masses in the region of $m_\pi \gtrsim$ (400–500) MeV we might have been tempted to assume also a linear behavior in the region of m_π down to the physical point. Such an extrapolation would have resulted in a surprizingly accurate estimate for the dipole masses of $M_2^Q(t)$ and $J^Q(t)$ at the physical point, see Fig. 8(a).

However, this procedure would have failed in the case of the dipole mass of $d_1^Q(t)$. In fact, also this dipole mass exhibits an approximately linear m_π behavior in the region $m_\pi \gtrsim 500$ MeV, see Fig. 8(a). But presuming that this linear behavior continues to hold also for $m_\pi \lesssim 500$ MeV would have resulted in a strong overestimate of the dipole mass of $d_1(t)$ at the physical point of about 30%, see Fig. 12.

Finally, let us discuss the m_π dependence of the form factor $d_1^Q(t)$ at zero momentum transfer. We observe an m_π behavior of $d_1^Q \equiv d_1^Q(0)$ in the region of $m_\pi > 400$ MeV which is linear to a very good approximation. However, if we assumed that this linear m_π-dependence continued down to small pion masses we would have underestimated the absolute value of d_1^Q at the physical point by about 25%, and in the chiral limit by 50%, see Fig. 12(b).

Recall that the chiral expansion of d_1^Q to linear order in m_π—i.e., up to the leading non-analytic contribution (in large N_c) according to Eq. (26)—approximates the full result rather

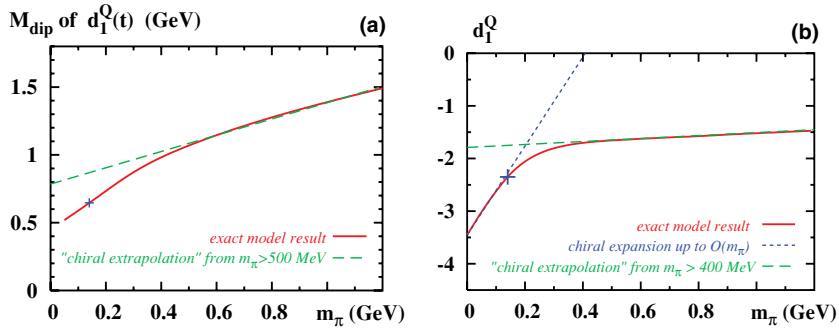

FIG. 12. (Color online) (a) The dipole mass $M_{\rm dip}$ of the form factor $d_1^Q(t)$ vs. m_π as obtained from the CQSM. The linear m_π dependence in the region $m_\pi \gtrsim 500\,\text{MeV}$ is emphasized. (b) The pion mass dependence of the constant d_1^Q as obtained from the CQSM at low scale. (Solid line) The exact result from the CQSM. (Dotted line) The chiral expansion of $d_1(m_\pi)$ to linear order in m_π according to Eq. (26). (Dashed line) The attempt of a "chiral extrapolation" from the region of large $m_\pi \gtrsim 400\,\text{MeV}$. In both figures the cross marks the physical point.

well up to the physical point. It is an interesting result that in our model d_1^Q exhibits in the region of large $m_\pi > 400\,\text{MeV}$ again a linear m_π dependence—just as at low $m_\pi \lesssim 140\,\text{MeV}$, however, with a roughly 30 times smaller slope!

Of course, we make these observations in an effective chiral theory formulated in the large N_c limit. The situation could be different in full QCD simulations performed at finite $N_c = 3$. However, the model was observed—in spite of its caveats like large vs. finite N_c—to provide a qualitatively good description of lattice results on the pion mass dependence of the nucleon mass in the region $300\,\text{MeV} \lesssim m_\pi \lesssim 1.5\,\text{GeV}$ [41]. Therefore it could be worth it to keep in mind the lessons we learn here from this model.

VIII. CONCLUSIONS

We have presented a study of the nucleon EMT form factors in the large-N_c limit in the framework of the CQSM in the region of pion masses $140\,\text{MeV} \leqslant m_\pi \leqslant 1.2\,\text{GeV}$. This work supplements the study of the nucleon EMT form factors in the region $0 \leqslant m_\pi \leqslant 140\,\text{MeV}$ [60]. There is a good reason why these studies have been presented separately. The CQSM [42,43] has been used extensively to study the nucleon at the physical point and in the chiral limit with considerable phenomenological success [46–59]. The model owes its success to the facts that it is a QCD-inspired field theoretic approach [72–74] which correctly describes chiral symmetry playing an essential role in the description of the nucleon.

Here we studied the CQSM at model parameters corresponding to large pion masses far above the physical point, i.e., far away from the chiral limit. Is the model applicable in this situation? First exploratory studies in this direction have indicated a positive answer [40,41]. To shed further light to this question we have focused here on the nucleon form factors of the EMT which is a central quantity for any field theoretic approach.

In our study we have demonstrated that the soliton solutions for large m_π obtained numerically in Ref. [41] correspond to stable solitons, which is an important prerequisite for the applicability of the approach. We have shown that the model results for the energy density, the angular momentum density, and the distributions of strong pressure and shear forces are in qualitative agreement with what one expects as the constituents building up the nucleon become heavy and the range of the pion cloud diminishes. Namely the spatial extension of the nucleon shrinks, the energy density increases, the absolute values of the forces inside the nucleon increase—resulting in a smaller and more tightly bound nucleon. These densities are related to the form factors of the EMT [3].

To test the model results in a more quantitative way we have compared them to results for the EMT form factors from lattice QCD simulations [24–28] performed at lattice parameters corresponding to $m_\pi \gtrsim 500\,\text{MeV}$. We observe a good agreement with the lattice data within an accuracy of (10–30)%. Also at the physical point the model was observed to work to within a similar accuracy [46–53].

The good performance of the model at the physical point and in the region of large pion masses raises the question whether the model results could be used as a guideline for the chiral extrapolation of lattice data. Given the generally observed accuracy of the model it is clear that it cannot be used as a precision extrapolation tool. However, the model results can be helpful in two respects.

First, our results can be of use as qualitative guidelines for the extrapolation of lattice data. For example, the model results indicate that the EMT form factors can be well approximated by dipole fits, and that the dipole masses of $M_2^Q(t)$ and $J^Q(t)$ exhibit to a good approximation a linear m_π dependence from $m_\pi = 1.2\,\text{GeV}$ down to the physical point. But our results indicate also that the chiral extrapolation of the form factor $d_1^Q(t)$ from the region $m_\pi \gtrsim (400\text{–}500)\,\text{MeV}$ could be a subtle and difficult task.

Second, the success of the model at large pion masses could provide a justification for applying the "pion cloud" idea to the description of nucleon up to pion masses of $\mathcal{O}(1\,\text{GeV})$ as explored in the finite range regulator approach. This approach may provide a useful and precise tool for the chiral extrapolation of lattice data as argued in Ref. [37,38].

To conclude, we observe that the CQSM provides a consistent description of the nucleon at large pion masses indicating that effective quark and pion degrees of freedom can account for the gross features of the nucleon properties also in this regime. Work which may provide further insigths in this direction is in progress.

Note added in proof. After this work was completed the work [91] appeared where the flavor dependence of the constant d_1 and its pion mass dependence were studied in a similar framework.

ACKNOWLEDGMENTS

We thank Philipp Hägler, Pavel Pobylitsa, Maxim Polyakov, and especially Wolfram Schroers for fruitful discussions and valuable comments. This research is part of the EU integrated infrastructure initiative hadron physics project under contract number RII3-CT-2004-506078 and partially supported by the Graduierten-Kolleg Bochum-Dortmund and Verbundforschung of BMBF. A.S. acknowledges support from GRICES and DAAD.

APPENDIX: ALTERNATIVE DEFINITION OF FORM FACTORS

By means of the Gordon identity $2M_N\bar{u}'\gamma^\alpha u = \bar{u}'(i\sigma^{\alpha\kappa}\Delta_\kappa + 2P^\alpha)u$ one can rewrite (1) as (see, e.g., in Ref. [5])

$$\langle p'|\hat{T}^{Q,G}_{\mu\nu}(0)|p\rangle = \bar{u}(p')\Big[A^{Q,G}(t)\,\frac{\gamma_\mu P_\nu + \gamma_\nu P_\mu}{2} + B^{Q,G}(t)\,\frac{i(P_\mu\sigma_{\nu\rho} + P_\nu\sigma_{\mu\rho})\Delta^\rho}{4M_N} + C^{Q,G}(t)\,\frac{\Delta_\mu\Delta_\nu - g_{\mu\nu}\Delta^2}{M_N} \pm \bar{c}(t)g_{\mu\nu}\Big] \times u(p), \tag{A1}$$

where $A^{Q,G}(t) = M_2^{Q,G}(t)$, $A^{Q,G}(t) + B^{Q,G}(t) = 2\,J^{Q,G}(t)$, $C^{Q,G}(t) = \frac{1}{5}\,d_1^{Q,G}(t)$. In this notation the constraints (8) read $A^Q(0) + A^G(0) = 1$ and $B^Q(0) + B^G(0) = 0$. The latter constraint is sometimes rephrased as the "vanishing of the total nucleon gravitomagnetic moment."

[1] H. R. Pagels, Phys. Rev. **144**, 1250 (1965).
[2] X. D. Ji, Phys. Rev. Lett. **78**, 610 (1997).
[3] M. V. Polyakov, Phys. Lett. **B555**, 57 (2003).
[4] D. Müller, D. Robaschik, B. Geyer, F. M. Dittes, and J. Hořejši, Fortschr. Phys. **42**, 101 (1994).
[5] X. D. Ji, Phys. Rev. D **55**, 7114 (1997).
[6] J. C. Collins, L. Frankfurt, and M. Strikman, Phys. Rev. D **56**, 2982 (1997).
[7] A. V. Radyushkin, Phys. Rev. D **56**, 5524 (1997).
[8] P. R. Saull (ZEUS Collaboration), in Proceedings of the International Europhysics Conference on High Energy Physics EPS-HEP 99, edited by K. Huitu, H. Kurki-Suonio, and J. Maalampi (IOP, Bristol, UK, 2000), p. 420 [arXiv:hep-ex/0003030].
[9] C. Adloff *et al.* (H1 Collaboration), Phys. Lett. **B517**, 47 (2001).
[10] A. Airapetian *et al.* (HERMES Collaboration), Phys. Rev. Lett. **87**, 182001 (2001).
[11] S. Stepanyan *et al.* (CLAS Collaboration), Phys. Rev. Lett. **87**, 182002 (2001).
[12] F. Ellinghaus (HERMES Collaboration), Nucl. Phys. **A711**, 171 (2002).
[13] S. Chekanov *et al.* (ZEUS Collaboration), Phys. Lett. **B573**, 46 (2003).
[14] A. Aktas *et al.* (H1 Collaboration), Eur. Phys. J. C **44**, 1 (2005).
[15] C. Munoz Camacho *et al.* (Jefferson Lab Hall A Collaboration), Phys. Rev. Lett. **97**, 262002 (2006) [arXiv:nucl-ex/0607029].
[16] A. Airapetian *et al.* (HERMES Collaboration), Phys. Rev. D **75**, 011103 (2007).
[17] X. D. Ji, J. Phys. G **24**, 1181 (1998).
[18] A. V. Radyushkin, in At the Frontier of Particle Physics, edited by M. Shifman (World Scientific, Singapore, 2001), Vol. 2, p. 1037 [arXiv:hep-ph/0101225].
[19] K. Goeke, M. V. Polyakov, and M. Vanderhaeghen, Prog. Part. Nucl. Phys. **47**, 401 (2001).
[20] A. V. Belitsky, D. Mueller, and A. Kirchner, Nucl. Phys. **B629**, 323 (2002).
[21] M. Diehl, Phys. Rep. **388**, 41 (2003).
[22] A. V. Belitsky and A. V. Radyushkin, Phys. Rep. **418**, 1 (2005).
[23] M. Burkardt, Phys. Rev. D **62**, 071503 (2000) [Erratum-*ibid.* **66**, 119903 (2002)]; M. Burkardt, Int. J. Mod. Phys. A **18**, 173 (2003); J. P. Ralston and B. Pire, Phys. Rev. D **66**, 111501 (2002); M. Diehl, Eur. Phys. J. C **25**, 223 (2002) [Erratum-*ibid.* **31**, 277 (2003)].
[24] N. Mathur, S. J. Dong, K. F. Liu, L. Mankiewicz, and N. C. Mukhopadhyay, Phys. Rev. D **62**, 114504 (2000).
[25] V. Gadiyak, X. Ji, and C. Jung, Phys. Rev. D **65**, 094510 (2002).
[26] P. Hägler, J. W. Negele, D. B. Renner, W. Schroers, T. Lippert, and K. Schilling (LHPC Collaboration), Phys. Rev. D **68**, 034505 (2003); Phys. Rev. Lett. **93**, 112001 (2004).
[27] M. Göckeler, R. Horsley, D. Pleiter, P. E. L. Rakow, A. Schäfer, G. Schierholz, and W. Schroers (QCDSF Collaboration), Phys. Rev. Lett. **92**, 042002 (2004).
[28] J. W. Negele *et al.*, Nucl. Phys. (Proc. Suppl.) **128**, 170 (2004).
[29] W. Schroers, Eur. Phys. J. A. **31**, 784 (2007) [arXiv:hep-lat/0701003]; Nucl. Phys. Proc. Suppl. **153**, 277 (2006) [arXiv:hep-lat/0512001]; R. G. Edwards *et al.*, arXiv:hep-lat/0610007.
[30] J. W. Chen and X. D. Ji, Phys. Rev. Lett. **88**, 052003 (2002).
[31] A. V. Belitsky and X. D. Ji, Phys. Lett. **B538**, 289 (2002).
[32] M. Diehl, A. Manashov, and A. Schäfer, Eur. Phys. J. A **29**, 315 (2006).
[33] V. Bernard, T. R. Hemmert, and U. G. Meissner, Nucl. Phys. **A732**, 149 (2004); V. Bernard, T. R. Hemmert, and U. G. Meissner, Phys. Lett. **B622**, 141 (2005); M. Frink and U. G. Meissner, JHEP 07 (2004), 028; M. Frink, U. G. Meissner, and I. Scheller, Eur. Phys. J. A **24**, 395 (2005).
[34] M. Procura, T. R. Hemmert, and W. Weise, Phys. Rev. D **69**, 034505 (2004) [arXiv:hep-lat/0309020]; M. Procura, B. U. Musch, T. R. Hemmert, and W. Weise, Phys. Rev. D **75**,014503 (2007) [arXiv:hep-lat/0610105].
[35] A. Ali Khan *et al.* (QCDSF-UKQCD Collaboration), Nucl. Phys. **B689**, 175 (2004); R. G. Edwards *et al.* (LHPC Collaboration), Phys. Rev. Lett. **96**, 052001 (2006).
[36] S. R. Beane, Nucl. Phys. **B695**, 192 (2004); J. A. McGovern and M. C. Birse, Phys. Rev. D **74**, 097501 (2006).
[37] D. B. Leinweber, D. H. Lu, and A. W. Thomas, Phys. Rev. D **60**, 034014 (1999); D. B. Leinweber, A. W. Thomas, K. Tsushima, and S. V. Wright, *ibid.* **61**, 074502 (2000); D. B. Leinweber, A. W. Thomas, and S. V. Wright, Phys. Lett. **B482**, 109 (2000); R. D. Young, D. B. Leinweber, A. W. Thomas, and S. V. Wright, Phys. Rev. D **66**, 094507 (2002); D. B. Leinweber,

A. W. Thomas, and R. D. Young, Phys. Rev. Lett. **92**, 242002 (2004); I. C. Cloet, D. B. Leinweber, and A. W. Thomas, Phys. Lett. **B563**, 157 (2003); R. D. Young, D. B. Leinweber, and A. W. Thomas, Phys. Rev. D **71**, 014001 (2005); C. R. Allton, W. Armour, D. B. Leinweber, A. W. Thomas, and R. D. Young, Phys. Lett. **B628**, 125 (2005).
[38] A. W. Thomas, Ann. Phys. **13**, 731 (2004).
[39] H. H. Matevosyan, G. A. Miller, and A. W. Thomas, Phys. Rev. C **71**, 055204 (2005); H. H. Matevosyan, A. W. Thomas, and G. A. Miller, *ibid*. **72**, 065204 (2005).
[40] P. Schweitzer, Phys. Rev. D **69**, 034003 (2004).
[41] K. Goeke, J. Ossmann, P. Schweitzer, and A. Silva, Eur. Phys. J. A **27**, 77 (2006) [arXiv:hep-lat/0505010].
[42] D. I. Diakonov and V. Y. Petrov, JETP Lett. **43**, 75 (1986) [Pisma Zh. Eksp. Teor. Fiz. **43**, 57 (1986)].
[43] D. I. Diakonov, V. Y. Petrov, and P. V. Pobylitsa, Nucl. Phys. **B306**, 809 (1988); D. I. Diakonov, V. Y. Petrov, and M. Praszałowicz, Nucl. Phys. **B323**, 53 (1989).
[44] E. Witten, Nucl. Phys. **B160**, 57 (1979); **B223**, 433 (1983).
[45] C. Schüren, E. Ruiz Arriola, and K. Goeke, Nucl. Phys. **A547**, 612 (1992).
[46] C. V. Christov, A. Z. Górski, K. Goeke, and P. V. Pobylitsa, Nucl. Phys. **A592**, 513 (1995).
[47] C. V. Christov *et al*., Prog. Part. Nucl. Phys. **37**, 91 (1996).
[48] A. Silva, H. C. Kim, D. Urbano, and K. Goeke, Phys. Rev. D **74**, 054011 (2006).
[49] D. I. Diakonov *et al*., Nucl. Phys. **B480**, 341 (1996).
[50] D. I. Diakonov, V. Y. Petrov, P. V. Pobylitsa, M. V. Polyakov, and C. Weiss, Phys. Rev. D **56**, 4069 (1997); P. V. Pobylitsa *et al*., *ibid*. **59**, 034024 (1999); P. V. Pobylitsa and M. V. Polyakov, Phys. Lett. **B389**, 350 (1996); C. Weiss and K. Goeke, arXiv:hep-ph/9712447.
[51] D. I. Diakonov, V. Y. Petrov, P. V. Pobylitsa, M. V. Polyakov, and C. Weiss, Phys. Rev. D **58**, 038502 (1998).
[52] M. Wakamatsu and T. Kubota, Phys. Rev. D **60**, 034020 (1999); M. Wakamatsu, *ibid*. **67**, 034005 (2003); **67**, 034006 (2003).
[53] K. Goeke *et al*., Acta Phys. Pol. B **32**, 1201 (2001); P. Schweitzer *et al*., Phys. Rev. D **64**, 034013 (2001).
[54] V. Y. Petrov, P. V. Pobylitsa, M. V. Polyakov, I. Börnig, K. Goeke, and C. Weiss, Phys. Rev. D **57**, 4325 (1998).
[55] M. Penttinen, M. V. Polyakov, and K. Goeke, Phys. Rev. D **62**, 014024 (2000).
[56] P. Schweitzer, S. Boffi, and M. Radici, Phys. Rev. D **66**, 114004 (2002).
[57] P. Schweitzer, M. Colli, and S. Boffi, Phys. Rev. D **67**, 114022 (2003); P. Schweitzer, S. Boffi, and M. Radici, Nucl. Phys. **A711**, 207 (2002).
[58] J. Ossmann, M. V. Polyakov, P. Schweitzer, D. Urbano, and K. Goeke, Phys. Rev. D **71**, 034011 (2005).
[59] M. Wakamatsu and H. Tsujimoto, Phys. Rev. D **71**, 074001 (2005); M. Wakamatsu and Y. Nakakoji, *ibid*. **74**, 054006 (2006).
[60] K. Goeke, J. Grabis, J. Ossmann, M. V. Polyakov, P. Schweitzer, A. Silva, and D. Urbano, Phys. Rev. D (2007), in press (arXiv:hep-ph/0702030).
[61] J. F. Donoghue and H. Leutwyler, Z. Phys. C **52**, 343 (1991).
[62] B. Kubis and U. G. Meissner, Nucl. Phys. **A671**, 332 (2000) [Erratum-*ibid*. **A692**, 647 (2001)].
[63] E. Megias, E. R. Arriola, L. L. Salcedo, and W. Broniowski, Phys. Rev. D **70**, 034031 (2004); E. Megias, E. Ruiz Arriola, and L. L. Salcedo, *ibid*. **72**, 014001 (2005).
[64] D. Brommel *et al*., PoS **LAT2005**, 360 (2006).
[65] J. W. Chen, W. Detmold, and B. Smigielski, Phys. Rev. D **75**, 074003 (2007) [arXiv:hep-lat/0612027].
[66] F. Ellinghaus, W. D. Nowak, A. V. Vinnikov, and Z. Ye, Eur. Phys. J. C **46**, 729 (2006) [arXiv:hep-ph/0506264].
[67] R. G. Sachs, Phys. Rev. **126**, 2256 (1962).
[68] M. V. Polyakov and C. Weiss, Phys. Rev. D **60**, 114017 (1999).
[69] O. V. Teryaev, Phys. Lett. **B510**, 125 (2001).
[70] N. Kivel, M. V. Polyakov, and M. Vanderhaeghen, Phys. Rev. D **63**, 114014 (2001).
[71] V. Guzey and M. Siddikov, J. Phys. G **32**, 251 (2006).
[72] D. I. Diakonov and V. Y. Petrov, Nucl. Phys. **B245**, 259 (1984).
[73] D. I. Diakonov and V. Y. Petrov, Nucl. Phys. **B272**, 457 (1986).
[74] D. I. Diakonov, M. V. Polyakov, and C. Weiss, Nucl. Phys. **B461**, 539 (1996).
[75] For reviews see: D. I. Diakonov, Prog. Part. Nucl. Phys. **51**, 173 (2003); D. I. Diakonov and V. Y. Petrov, in *At the Frontier of Particle Physics*, edited by M. Shifman (World Scientific, Singapore, 2001), Vol. 1, p. 359–415.
[76] D. I. Diakonov and M. I. Eides, JETP Lett. **38**, 433 (1983) [Pisma Zh. Eksp. Teor. Fiz. **38**, 358 (1983)].
[77] A. Dhar, R. Shankar, and S. R. Wadia, Phys. Rev. D **31**, 3256 (1985).
[78] S. Kahana and G. Ripka, Nucl. Phys. **A429**, 462 (1984).
[79] T. Kubota, M. Wakamatsu, and T. Watabe, Phys. Rev. D **60**, 014016 (1999).
[80] P. V. Pobylitsa, E. Ruiz Arriola, T. Meissner, F. Grummer, K. Goeke, and W. Broniowski, J. Phys. G **18**, 1455 (1992).
[81] R. F. Dashen, E. Jenkins, and A. V. Manohar, Phys. Rev. D **49**, 4713 (1994) [Erratum-*ibid*. **51**, 2489 (1995)].
[82] T. D. Cohen and W. Broniowski, Phys. Lett. **B292**, 5 (1992); T. D. Cohen, arXiv:hep-ph/9512275.
[83] S. L. Adler, J. C. Collins, and A. Duncan, Phys. Rev. D **15**, 1712 (1977); N. K. Nielsen, Nucl. Phys. **B120**, 212 (1977); J. C. Collins, A. Duncan, and S. D. Joglekar, Phys. Rev. D **16**, 438 (1977).
[84] V. M. Braun, P. Górnicki, L. Mankiewicz, and A. Schäfer, Phys. Lett. **B302**, 291 (1993).
[85] See, for example, M. Glück and E. Reya, Nucl. Phys. **B130**, 76 (1977), and references therein.
[86] M. Glück, E. Reya, and A. Vogt, Z. Phys. C **67**, 433 (1995).
[87] M. Glück, E. Reya, and A. Vogt, Eur. Phys. J. C **5**, 461 (1998).
[88] A. V. Efremov, K. Goeke, and P. V. Pobylitsa, Phys. Lett. **B488**, 182 (2000).
[89] For examples of other large-N_c results and their tests see: P. V. Pobylitsa, arXiv:hep-ph/0301236; A. V. Efremov, K. Goeke, S. Menzel, A. Metz, and P. Schweitzer, Phys. Lett. **B612**, 233 (2005); J. C. Collins, A. V. Efremov, K. Goeke, S. Menzel, A. Metz, and P. Schweitzer, Phys. Rev. D **73**, 014021 (2006).
[90] O. V. Teryaev, arXiv:hep-ph/9803403, and arXiv:hep-ph/9904376.
[91] M. Wakamatsu, Phys. Lett. B **648**, 181 (2007) [arXiv:hep-ph/0701057].